SCUOLA INTERNAZIONALE SUPERIORE DI STUDI AVANZATI

SISSA Digital Library

Lindblad dissipative dynamics in the presence of phase coexistence

(Article begins on next page)

09 March 2020

Lindblad dissipative dynamics in presence of phase coexistence

Andrea Nava[1] and Michele Fabrizio[1]

[1]*International School for Advanced Studies (SISSA), Via Bonomea 265, I-34136 Trieste, Italy*

We investigate the dissipative dynamics yielded by the Lindblad equation within the coexistence region around a first order phase transition. In particular, we consider an exactly-solvable fully-connected quantum Ising model with n-spin exchange ($n > 2$) – the prototype of quantum first order phase transitions – and several variants of the Lindblad equations. We show that physically sound results, including exotic non-equilibrium phenomena like the Mpemba effect, can be obtained only when the Lindblad equation involves jump operators defined for each of the coexisting phases, whether stable or metastable.

PACS numbers:

I. INTRODUCTION

Even if it covers 71% of the earth surface and more than half of human body is made of it, water still represents a scientific challenge for its fascinating and intriguing physical properties[1,2], among which its anomalous relaxation time, revealed, e.g., by hot buckets of water freezing faster than colder ones, both exposed to the same subzero environment. This counter intuitive effect, already known by Aristotle, Bacon and Descartes, was formalized only in 1969 by the high school student Erasto Batholomeo Mpemba in the attempt to freeze a hot ice cream mixture[3], after him named Mpemba effect. Although the existence of such phenomenon in water has been questioned[4], it has actually been observed also in clathrate hydrates[5], magneto-resistance alloys[6], granular systems[7] and spin glasses[8]. Several proposals have been formulated to explain how and when the Mpemba effect may or not take place, which invoke properties of the hydrogen bonds[9], evaporation[10,11], conduction and convection[12], and, eventually, the supercooling process[13,14].

Usually, liquid water cooled down to the freezing temperature 273.15 K starts to crystallize around nucleation sites. As discovered by D. G. Fahrenheit in 1724[15], in pure, i.e, free of impurities, water it is possible to delay by a proper cooling procedure the formation of ice nucleators, and thus the freezing, till temperatures of the order of 231.15 K, the liquid spinodal temperature. Supercooled water remains trapped in the liquid metastable state for quite a long time before spontaneously crystallising in the stable solid phase, unless shaken. When supercooling is realized during a fast process, like a quench, the Newton's heat law may not apply and the Mpemba effect occur. Specifically, in the free-energy landscape corresponding to the solid-liquid coexistence region, a system cooled down from a lower temperature could fall in the metastable minimum with higher probability and remain trapped there for a longer time than a system cooled down from a higher temperature.

At low temperature, a faithful description of super-cooling, and its associated phenomena like, e.g., the Mpemba effect, can do without proper modelling of the quantum dissipative dynamics in presence of phase coexistence. In this work we shall address right this issue in the prototype quantum first order phase transition displayed by a fully connected quantum Ising model with p-spin exchange, where $p > 2$.

Quantum spin models, besides being paradigmatic systems for studying quantum phase transitions, also constitute a good playground to investigate, both theoretically and experimentally, the driven dissipative dynamics[16–24]. We shall model the dissipative dynamics of our case study in the framework of Markovian dynamics, through the rather general master equation derived by Lindblad back in 1976[25,26], but still widely used[27–34]. As a matter of fact, metastability in Markovian open quantum systems turns out to be a non trivial problem[35] due to the separation of timescales in the dissipative dynamics[36]. Typically, the Lindblad equation is able to describe the short time dynamics during which the system relaxes to a metastable state[37–39], while it fails to describe the long time ergodic dynamics that drives relaxation to the true equilibrium state.

Here, we show how to describe the full dynamics in terms of an effective Lindblad equation valid in both regimes. The main idea is to write the master equation as a sum of competing terms, one for each phase within the metastable manifold. Within this description both supercooling and Mpemba effect spontaneously emerges during the quantum dissipative dynamics.

The paper is organized as follows. In Section II we introduce the quantum Ising model we shall investigate and its equilibrium phase diagram. In Section III we briefly discuss the Lindblad master equation to describe the Markovian relaxation dynamic, and consider the simple case of a single spin-$1/2$ in a static or dynamic magnetic field. In Section IV we specialise the Lindblad equation in the fully connected quantum Ising model, and show how it can be exploited to recover the equilibrium phase diagram. In Section V we present a variant of the Lindblad equation appropriate in case of phase coexistence, and apply it to our quantum Ising model, which
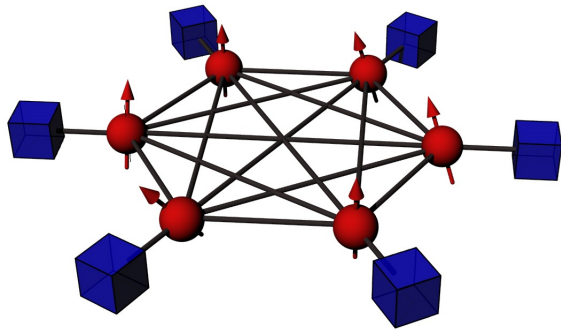
FIG. 1. Graphic representation of the model: a fully connected graph of N spins (red balls), here shown for $N = 6$, each in contact with its own bath (blue boxes).

indeed shows Mpemba effect. Finally, Sec. VI is devoted to concluding remarks.

II. THE MODEL HAMILTONIAN

We wish to describe the dynamics of an open quantum system, which must be as simple as possible but still posses a non-trivial phase diagram with metastable phases. For that purpose, we consider a quantum Ising model on an N-sites fully connected graph, sketched in Fig. 1 for $N = 6$, described by the Hamiltonian

$$H = -h_x \sum_i \sigma_i^x - N \sum_{n=2}^m J_n \left(\frac{1}{N} \sum_i \sigma_i^z \right)^n , \quad (1)$$

with integer $m \geq 2$. Here σ_i^α, $\alpha = x, y, z$, are Pauli matrices on site $i = 1, \ldots, N$, h_x a transverse magnetic field, and J_n n-spin exchange constants.

Hereafter, we shall focus on three reference cases that are representative of all others. Specifically,

1. $J_2 \neq 0$, $J_4 \neq 0$, and $J_{n \neq 2,4} = 0$;

2. $J_3 \neq 0$ and $J_{n \neq 3} = 0$;

3. $J_2 \neq 0$ and $J_{n \neq 2} = 0$.

In all three cases the model undergoes a phase transition increasing either temperature T or transverse field h_x from a phase with finite to one with vanishing expectation value of σ_i^z, $\forall$ i. This transition is first order in case $1^{33,40}$ and 2^{41}, but second order in case 3^{31}. Moreover, in case 1 and 3 it corresponds to the restoration of the Z_2 symmetry $\sigma_i^z \rightarrow -\sigma_i^z$, $\forall$ i, which is spontaneously broken in the low T and h_x phase, while such symmetry is explicitly broken in case 2.

Because of full connectivity, mean-field approximation becomes exact for model (4) in the thermodynamic limit $N \rightarrow \infty$, since, for $i \neq j$, and for any $\alpha, \beta = x, y, z$,

$$\langle \sigma_i^\alpha \sigma_j^\beta \rangle - \langle \sigma_i^\alpha \rangle \langle \sigma_j^\beta \rangle \propto \frac{1}{N} \xrightarrow[N \to \infty]{} 0 . \quad (2)$$
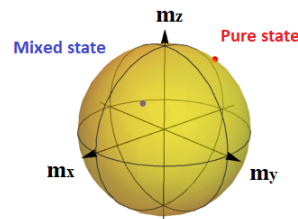

FIG. 2. Effective 2-d Bloch sphere for the mean values of the spin components

It follows that the equilibrium Boltzmann distribution

$$\rho = \frac{e^{-\beta H}}{\text{Tr}\left(e^{-\beta H}\right)} \xrightarrow[N \to \infty]{} \prod_i \rho_i = \prod_i \frac{e^{-\beta H_i}}{\text{Tr}\left(e^{-\beta H_i}\right)} , \quad (3)$$

where $\beta = 1/T$ and the local mean field Hamiltonian reads

$$H_i = -h_x \sigma_i^x - h_z(\mathbf{m}) \sigma_i^z . \quad (4)$$

The longitudinal field in (4) is defined by

$$h_z(\mathbf{m}) = \sum_{n=2}^m n J_n m_z^{n-1} , \quad (5)$$

where $\mathbf{m} = (m_x, m_y, m_z)$ is the Bloch vector with components

$$m_\alpha \equiv \frac{1}{N} \sum_j \langle \sigma_j^\alpha \rangle , \quad \alpha = x, y, z . \quad (6)$$

The local density matrix ρ_i in Eq. (3) can be also written as the 2×2 matrix

$$\rho_i = \frac{1}{2}\left(1 + \mathbf{m} \cdot \boldsymbol{\sigma}_i\right) , \quad (7)$$

where $\boldsymbol{\sigma}_i = (\sigma_i^x, \sigma_i^y, \sigma_i^z)$, and it is completely determined by the Bloch vector $\mathbf{m}$. In general $|\mathbf{m}| \leq 1$, being $|\mathbf{m}| = 1$ only for pure states (see Fig. 2). Assuming the system at equilibrium with a bath at at temperature T, the expectation values in (7) read

$$\mathbf{m} = \tanh\left(\beta h(\mathbf{m})\right)\left(\cos\theta(\mathbf{m}), 0, \sin\theta(\mathbf{m})\right), \quad (8)$$

where

$$\tan\theta(\mathbf{m}) = \frac{h_z(\mathbf{m})}{h_x} , \quad (9)$$
$$h(\mathbf{m}) = \sqrt{h_x^2 + h_z(\mathbf{m})^2} .$$

Eqs. (8) and (9) self-consistently determine the equilibrium state at temperature T, leading to the phase diagram shown in Fig. 3 for the three different cases. In the figure, F denotes the ferromagnetic phase with $m_z \neq 0$, P the paramagnetic one with $m_z = 0$, while FP and PF the coexistence regions, FP with F stable and P metastable and PF vice versa.
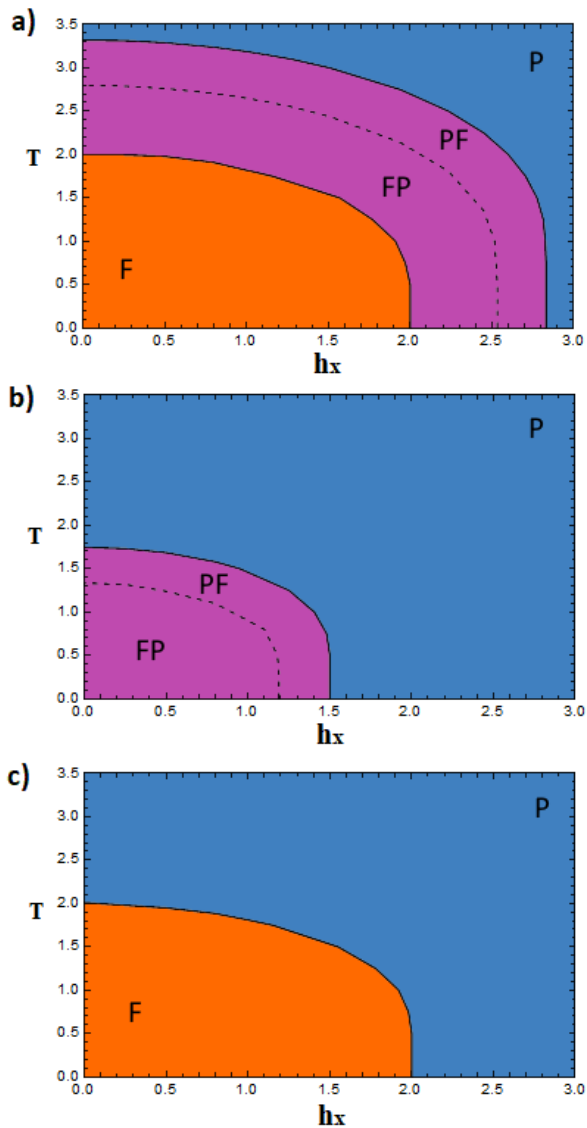
FIG. 3. Phase diagram of the Hamiltonian (4) in case 1 with $J_2 = J_4 = 1$, panel a), case 2 with $J_3 = 1$, panel b), and case 3 with $J_2 = 1$, panel c). The label F stand for the ferromagnetic phase with $m_z \neq 0$, P for the paramagnetic one with $m_z = 0$. FP denotes the coexistence region where the stable phase is F and the metastable P; the opposite case is denoted as PF. The first order transition between FP and PF in panels a) and b) is indicated as a dashed line, while the direct F to P transition in panel c) is a second order one. The F/FP and PF/P lines are, respectively, the P and F spinodal lines.

III.   LINDBLAD EQUATION

The dynamics of open quantum systems is usually described through a master equation, aimed to represent the true quantum evolution after integrating out the bath degrees of freedom. The derivation of such equation usually relies on the so-called Markovian approximation, which consists of neglecting memory effects

under the assumption that the bath relaxation-time is much shorter than the characteristic time-scales of the system. The Lindblad equation is among the most used master equations[25]. It can be derived in various ways and under different assumptions, like, e.g., the quantum dynamical semigroups formalism, the Ito stochastic calculus[42], the projector techniques associated to the rotating wave approximation[43] or the Keldysh diagrammatic formalism[44,45].

If the Born approximation is valid, i.e., if we can safely neglect system-bath correlations, the system (S) + bath (B) density matrix can be written as a tensor product

$$\rho_{S+B}(t) \simeq \rho_S(t) \otimes \rho_B(t). \tag{10}$$

The general form of the Lindblad equation consists in a first-order differential equation for the time evolution of the system density matrix $\rho_S(t)$:

$$\dot{\rho}(t)_S = -i \left[H_S , \rho_S(t) \right]$$
$$+ \sum_\lambda \left[\gamma_\lambda \left(2 L_\lambda \rho_S L_\lambda^\dagger - \left\{ L_\lambda^\dagger L_\lambda , \rho_S \right\} \right) \right], \tag{11}$$

where H_S is the system Hamiltonian and L_λ are the so-called Lindblad or jump operators, which are determined by the coupling between the system and the bath, and span the space of all independent operators within the system Hilbert space. The first term in the Lindblad equation (11) is the so-called Liouvillian that describes the unitary evolution brought by H_S, while the second term, so-called Lindbladian, includes dissipation and decoherence in the dynamics. Neglecting pure dephasing processes, the relaxation dynamics of a system is described by non-hermitian jump operators that produce transitions between the eigenstates $|n\rangle$ of H_S with eigenvalues E_n. Specifically, we shall define[26]

$$L_{\lambda(m,n)} = |m\rangle \langle n|, \quad E_n < E_m. \tag{12}$$

Using such definition of L_λ, we can write Eq. (11) as

$$\dot{\rho}_S = -i \left[H_S , \rho_S \right] + \sum_\lambda \left[\vphantom{\sum} \right.$$
$$\gamma_\lambda \left(2 L_\lambda \rho_S L_\lambda^\dagger - \left\{ L_\lambda^\dagger L_\lambda , \rho_S \right\} \right) \tag{13}$$
$$\left. + \bar{\gamma}_\lambda \left(2 L_\lambda^\dagger \rho_S L_\lambda - \left\{ L_\lambda L_\lambda^\dagger , \rho_S \right\} \right) \right].$$

One can readily verify that the Boltzmann distribution is a stationary solution of (13) if the coupling constants γ_λ and $\bar{\gamma}_\lambda$ are related to each other through

$$\frac{\bar{\gamma}_\lambda}{\gamma_\lambda} = e^{\beta \epsilon_\lambda}, \tag{14}$$

where $\epsilon_\lambda = E_m - E_n > 0$ are excitation energies. In what follows, we shall use the Lindblad equation (13) with the condition (14).

A. A single spin-1/2 in a magnetic field

As an example, useful in the next discussion of the Hamiltonian (4), let us consider the paradigmatic case of a single spin-1/2 in a magnetic field, with Hamiltonian

$$H_S = -\mathbf{h} \cdot \boldsymbol{\sigma} = -|\boldsymbol{h}| \, \boldsymbol{v}_3 \cdot \boldsymbol{\sigma} \,, \qquad (15)$$

where $\boldsymbol{v}_3 \,\|\, \boldsymbol{h}$ is a unit vector, coupled to a dissipative bath at temperature T. In this simple case, the ground state of H_S satisfies the eigenvalue equation $H_S \,|\,0\rangle = -|\mathbf{h}| \,|\,0\rangle$, and there is a single excited state, $|\,1\rangle$, at energy $\epsilon = 2|\mathbf{h}|$ above. It follows that there is only one jump operator defined through Eq. (12), namely

$$L = |1\rangle\langle 0| = \big(\boldsymbol{v}_1 - i\,\boldsymbol{v}_2\big) \cdot \boldsymbol{\sigma}/2 \equiv \boldsymbol{v}^- \cdot \boldsymbol{\sigma}/2 \,, \qquad (16)$$

with $\epsilon_\lambda = 2|\boldsymbol{h}|$, where $\boldsymbol{v}_1$ and $\boldsymbol{v}_2$ are real orthogonal unit vectors satisfying $\boldsymbol{v}_1 \wedge \boldsymbol{v}_2 \cdot \boldsymbol{v}_3 = 1$. Plugging L, and its hermitian conjugate,

$$L^\dagger = |0\rangle\langle 1| = \big(\boldsymbol{v}_1 + i\,\boldsymbol{v}_2\big) \cdot \boldsymbol{\sigma}/2 \equiv \boldsymbol{v}^+ \cdot \boldsymbol{\sigma}/2 \,, \qquad (17)$$

into Eq. (13) and computing the expectation values of the spin operator we obtain the Lindblad equation for the magnetisation $\mathbf{m}(t)$, namely,

$$\begin{aligned}
\dot{\boldsymbol{m}}(t) \equiv \mathrm{Tr}\Big(\dot{\rho}_S(t)\,\boldsymbol{\sigma}\Big) = &-2\boldsymbol{h} \wedge \boldsymbol{m}(t) \\
&- \frac{\gamma}{2}\Big[4\big(\boldsymbol{v}_3 + \mathbf{m}(t)\big) - \boldsymbol{v}^-\big(\boldsymbol{v}^+ \cdot \mathbf{m}(t)\big) \\
&\hspace{3.5em} - \boldsymbol{v}^+\big(\boldsymbol{v}^- \cdot \mathbf{m}(t)\big)\Big] \\
&+ \frac{\bar{\gamma}}{2}\Big[4\big(\boldsymbol{v}_3 - \mathbf{m}(t)\big) + \boldsymbol{v}^-\big(\boldsymbol{v}^+ \cdot \mathbf{m}(t)\big) \\
&\hspace{3.5em} + \boldsymbol{v}^+\big(\boldsymbol{v}^- \cdot \mathbf{m}(t)\big)\Big] \,.
\end{aligned} \qquad (18)$$

The stationary solution correctly reproduces the thermal equilibrium, $\mathbf{m}\cdot\boldsymbol{v}_3 = \tanh(\beta\,|\boldsymbol{h}|)$, and $\mathbf{m}\cdot\boldsymbol{v}_1 = \mathbf{m}\cdot\boldsymbol{v}_2 = 0$. Eq. (18) allows following the system evolution within the Bloch sphere from an arbitrary initial condition to the equilibrium stationary state.

Let us consider now the same system Hamiltonian but now in presence of a time dependent magnetic field

$$H_S\big(\boldsymbol{h}(t)\big) = -\boldsymbol{h}(t)\cdot\boldsymbol{\sigma} = -|\boldsymbol{h}(t)|\,\boldsymbol{v}_3(t)\cdot\boldsymbol{\sigma}\,, \qquad (19)$$

where $\boldsymbol{h}(t)$ evolves from an initial value, $\boldsymbol{h}(t \leq 0) = \boldsymbol{h}_i$, to a final one, $\boldsymbol{h}(t \gg 1) = \boldsymbol{h}_f$. A possible choice of the Lindblad operator that guarantees relaxation to the equilibrium density matrix ρ_{Sf} of the final Hamiltonian $H_S\big(\boldsymbol{h}_f\big)$ is the one in Eq. (12) defined through the eigenstates of the instantaneous Hamiltonian, i.e., from Eq. (16),

$$L(t) = \boldsymbol{v}^-(t)\cdot\frac{\boldsymbol{\sigma}}{2}\,, \quad L^\dagger(t) = \boldsymbol{v}^+(t)\cdot\frac{\boldsymbol{\sigma}}{2}\,, \qquad (20)$$

where $\boldsymbol{v}^+(t) = \boldsymbol{v}^-(t)^*$, which satisfy

$$\boldsymbol{v}^+(t) \wedge \boldsymbol{v}^-(t) = 2\boldsymbol{v}_3(t)\,. \qquad (21)$$

The Lindblad equation is the same as in Eq. (18), though with time dependent $\boldsymbol{v}^\pm(t)$ and $\epsilon_\lambda(t) = 2|\boldsymbol{h}(t)|$ in (14). In reality, the precise time dependence of the Lindblad operator $L(t)$ is not crucial to guarantee relaxation to the equilibrium ρ_{Sf}; what actually matters is just that $L(t)$ becomes, for $t \gg 1$, the Lindblad operator (16) corresponding to the final Hamiltonian $H_s(\boldsymbol{h}_f)$.

IV. DYNAMICS IN THE FULLY CONNECTED QUANTUM ISING MODEL

Let us consider a generic model in contact with a bath and subject to a quench of the state variables or of the Hamiltonian parameters, such that its phase diagram with the final system parameters comprises metastable phases besides the stable one. In this case, the proper choice of the Lindblad operators that could describe equally well the approach to equilibrium and non equilibrium phenomena like, e.g., supercooling or superheating, is not so straightforward. For instance, the most natural choice of Lindblad operators defined as in Eq. (12) through the eigenstates of the final Hamiltonian at the final values of the state variables does yield relaxation to equilibrium, but cannot produce trapping in a metastable phase.

We shall tackle precisely this issue in the simple model Hamiltonian (4). Here, full connectivity ensures that also the time-dependent density matrix of the system becomes factorizable in the thermodynamic limit, $N \to \infty$, namely,

$$\rho_S(t) \;\underset{N\to\infty}{\longrightarrow}\; \prod_i \rho_i(t)\,, \qquad (22)$$

where $\rho_i(t)$ describes the time evolution of the spin at site i coupled to a bath at temperature T and in presence of an effective time dependent magnetic field, exactly like the Hamiltonian (19). The difference with the latter is that, through (5), the field

$$\begin{aligned}
\boldsymbol{h}(t) = \boldsymbol{h}\big(\mathbf{m}(t)\big) &= \Big(h_x\,,\, 0\,,\, \sum_{n=2}^{m} n\,J_n\,m_z(t)^{n-1}\Big) \\
&\equiv \big|\boldsymbol{h}\big(\mathbf{m}(t)\big)\big|\,\boldsymbol{v}_3\big(\mathbf{m}(t)\big)\,,
\end{aligned} \qquad (23)$$

with

$$\mathbf{m}(t) = \frac{1}{N}\sum_i \mathrm{Tr}\Big(\rho_S(t)\,\boldsymbol{\sigma}_i\Big)\,, \qquad (24)$$

is self-consistently determined by the system time evolution, and thus the Lindblad equation acquires non-linear terms.

In this case we have several options for choosing the Lindblad jump operators. For instance, we may define $L(t)$ by the eigenstates of the instantaneous system Hamiltonian, namely using the expression in Eq. (20), where $\boldsymbol{v}_3(t)$ in

Eq. (21) is defined by Eq. (23) and $\epsilon_\lambda = 2|\boldsymbol{h}(\mathbf{m}(t))|$. This is however not the only choice, as there are several alternative definitions of the jump operators. We already showed in Sec. II that the free energy of the model Hamiltonian (4) has different minima, characterised by different values $m_z^{(a)}$, $a = 1, \ldots,$ of m_z, and thus each of them associated with a different effective field

$$\boldsymbol{h}^{(a)} = \left(h_x, \, 0, \, \sum_{n=2}^{m} n \, J_n \, m_z^{(a)n-1} \right) \equiv \left| \boldsymbol{h}^{(a)} \right| \boldsymbol{v}_3^{(a)}. \quad (25)$$

We can thus choose as jump operators those associated with the free energy minima $a = 1, \ldots,$ namely,

$$L^{(a)} = \boldsymbol{v}^{(a)-} \cdot \frac{\boldsymbol{\sigma}}{2}, \quad L^{(a)\dagger} = \boldsymbol{v}^{(a)+} \cdot \frac{\boldsymbol{\sigma}}{2}, \quad (26)$$

where

$$\boldsymbol{v}^{(a)+} \wedge \boldsymbol{v}^{(a)-} \equiv \left(\boldsymbol{v}^{(a)-} \right)^* \wedge \boldsymbol{v}^{(a)-} = 2\boldsymbol{v}_3^{(a)}, \quad (27)$$

and Eq. (14) with

$$\epsilon_\lambda = \epsilon_a = 2 \left| \boldsymbol{h}^{(a)} \right|. \quad (28)$$

In what follows, we analyse strengths and weaknesses of $L(t)$ defined through the eigenstates of the instantaneous Hamiltonian, while in the next section we shall present an alternative definition based on the jump operators (26) that yields physically more sound dynamics in presence of metastable phases.

A. Jump operator defined through the instantaneous Hamiltonian

We study first the dynamical evolution with the jump operator $L(t)$ defined through the equations (20), (23) and (21). The Lindblad equation for the average magnetisation $\mathbf{m}(t)$ is the same as in Eq. (18), with time dependent $\boldsymbol{h}(\mathbf{m}(t))$ and $\boldsymbol{v}^\pm(\mathbf{m}(t))$. One readily realises that the stationary solutions of that equation, including or not the Liouvillian, i.e., the first term on the r.h.s. of Eq. (18), correspond to the extrema of the free energy. The magnetisation $\mathbf{m}(t)$ thus flows towards one of those extrema depending on the initial conditions. More rigorously, $\mathbf{m}(t)$ flows towards one of the minima, unless it is initially right on a saddle point. We can therefore integrate numerically Eq. (18) starting from any initial condition and, by doing so, map out all basins of attraction within the Bloch sphere, which is actually the same as calculating the phase diagram.

In Figs. 4 and 5 we show the basins of attraction of Eq. (18) discarding and including, respectively, the Liouvillian, at very small T and in the three cases of interest. Considering for instance case 1, we note at small h_x two basins of attraction at finite and opposite values of m_z, which signal the Z_2 symmetry broken phase. The three basins for intermediate values of h_x indicate instead the
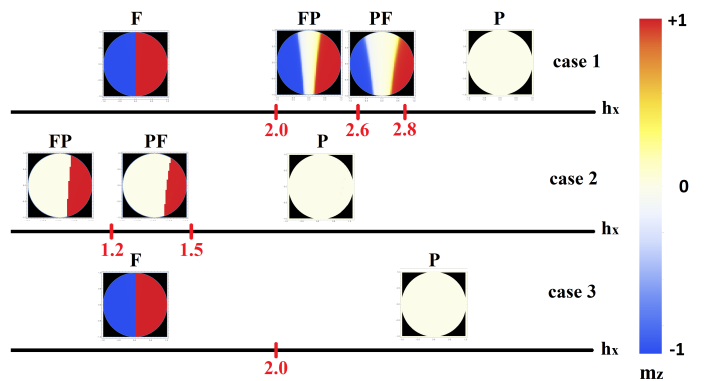

FIG. 4. Basins of attraction of the Lindblad equation neglecting the Liouvillian for the magnetisation $\mathbf{m}(t)$ within the Bloch sphere projected onto the $m_y = 0$ plane and for $T \to 0$. Top panel: case 1 with $J_2 = J_4 = 1$. Middle panel: case 2 with $J_3 = 1$. Bottom panel: case 3 with $J_2 = 1$. The colours indicate the stationary value of the longitudinal magnetisation m_z; specifically, red means $m_z > 0$, blue $m_z < 0$ and white $m_z = 0$.
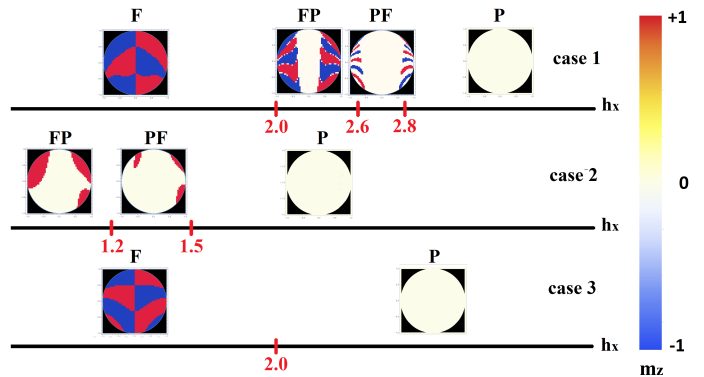

FIG. 5. Same as Fig. 4 including the Liouvillian. Note that apparently disconnected regions with the same colour are actually connected along the y-direction.

coexistence regions, FP or PF. Finally, at large h_x there is only one basin with $m_z = 0$. Repeating the above analysis at any temperature, we can obtain the same phase diagrams of Fig. 3.

We end noting that, while the Lindblad jump operator defined through the eigenstates of the instantaneous Hamiltonian provides an alternative and efficient way to calculate the phase diagram, it fails to produce relaxation to equilibrium. Indeed, when the system starts in the basin of attraction of a metastable phase, it will remain trapped there forever, at least in our simple model (4).

V. LINDBLAD OPERATORS IN PRESENCE OF PHASE COEXISTENCE

The unsatisfying results in Sec. IV A call for a different definition of jump operators able to describe the expected relaxation to equilibrium even in presence of metastable phases. For that, we observe that the Hilbert space of a system that undergoes phase transitions comprises several disconnected subspaces. The thermodynamic properties at given temperature and Hamiltonian parameters is determined just by one of those subspaces at a time. Let us consider, as an example, a system whose phase diagram looks like panel c) in Fig. 3, which displays a second order transition into a broken symmetry phase. In this case the Hilbert space in the thermodynamic limit decomposes into two subspaces; one that includes the symmetry invariant eigenstates, and the other the symmetry variant ones. The latter is in turn further decomposed into sub subspaces, also disconnected in the thermodynamic limit, and related one to the other by the generators of the symmetry that is spontaneously broken. A similar decomposition holds also when the transition is first order, like in cases 1 and 2 of the Hamiltonian (4), whose phase diagrams are shown in panels a) and b), respectively, of Fig. 3. The difference here is that the disconnected subspaces overlap in energy, thus the coexistence regions.

In all these situations it is rather natural to introduce jump operators of the form in Eq. (12) within each subspace, since different subspaces are disconnected from each other. In a dissipative environment, each subspace will act as a basin of attraction of the dynamics, which implies that the Lindblad equation would generally include jump operators of all subspaces, namely

$$
\begin{aligned}
\dot{\rho}_S = -i\Big[H_S\,,\rho_S\Big] + \sum_a \alpha_a(t) \sum_\lambda \Bigg[\\
\gamma_\lambda^{(a)}\Big(2L_\lambda^{(a)}\,\rho_S\,L_\lambda^{(a)\dagger} - \Big\{L_\lambda^{(a)\dagger}\,L_\lambda^{(a)}\,,\rho_S\Big\}\Big) \\
+ \bar{\gamma}_\lambda^{(a)}\Big(2L_\lambda^{(a)\dagger}\,\rho_S\,L_\lambda^{(a)} - \Big\{L_\lambda^{(a)}\,L_\lambda^{(a)\dagger}\,,\rho_S\Big\}\Big)\Bigg].
\end{aligned}
\tag{29}
$$

where $a = 1,\dots$ labels the subspaces, and the coefficient $\alpha_a(t)$ weighs the attraction strength of subspace a. Physically, we expect that $\alpha_a(t)$ is (1) smaller for subspaces that correspond to metastable phases than for those corresponding to stable ones; and (2) smaller the closer the system instantaneously is to the basin of attraction of another subspace. These two features guarantee that the system does flow to the equilibrium stable phase, unless it happens to be deep in the basin of attraction of a metastable phase, and thus remedy the drawbacks of the infinite lifetimes of metastable phases highlighted in Sec. IV A, without spoiling supercooling or superheating. Incidentally, we note that choosing $\alpha_a(t) = 1$ and $\alpha_{b\neq a} = 0$ in Eq. (29) brings to a steady state trapped into the subspace a, even if it not the equilibrium one.

In the simple case of the mean-field Hamiltonian (4), the different subspaces actually corresponds to the different minima of the free energy that we have discussed in Sec. IV. Moreover, the above requirements (1) and (2) can be easily implemented. For instance, we may assume for the coefficients $\alpha_a(t)$ in Eq. (29) the expression

$$
\alpha_a(t) = \Gamma\,\mathrm{e}^{-\beta f_a} \prod_{b\neq a}\Big(1 - \boldsymbol{v}_3\big(\mathbf{m}(t)\big)\cdot\boldsymbol{v}_3^{(b)}\Big).
\tag{30}
$$

Here Γ determines the overall strength of the coupling with the bath, while $\boldsymbol{v}_3\big(\mathbf{m}(t)\big)$ and $\boldsymbol{v}_3^{(a)}$ are defined in equations (23) and (25), respectively, and implement the condition (1). Finally, $\mathrm{e}^{-\beta f_a}$ is an Arrhenius term that involves the free energy per site f_a of the minimum a, and enforces the condition (2).

A. Mpemba effect

The Lindblad equation (29), with $\alpha_a(t)$ defined in Eq. (30), yields a physically sound dissipative dynamics of the Hamiltonian (4), including also the Mpbemba effect discussed in the Introduction. For that, let us consider the Hamiltonian (4) in case 1 with $J_2 = J_4 = 1$ and $h_x = 2.5$, see panel a) in Fig. 3. We assume two copies, one initially at equilibrium with a bath at temperature $T_{i,1}$, and the other at temperature $T_{i,2}$, with $T_{i,1} < T_{i,2}$ and both above the F spinodal point $T_{sF} \simeq 2.4$. Therefore, at first both copies are in the P phase, panel a) in Fig. 3. We then quench both systems to the same final temperature T_f that falls into the FP coexistence region, with the ferromagnetic phase stable and the paramagnetic one metastable. In order to seed nucleation of the F phase within the P one, we assume initially a tiny but finite $m_z = 0.05$.

In Fig. 6 we show the time evolution obtained by integrating the Lindblad equation of the longitudinal magnetisation m_z, top panel, and transverse magnetisation m_x, bottom panel, both for the initially hotter (red lines) and colder (blue lines) copies. We observe a quite long transient where both copies remain trapped into the P phase they started from, metastable at the final temperature, which can thus be viewed as a supercooled P phase. However, the hotter copy gets out of the metastable P phase, and fast reaches thermalisation, earlier than the colder one; this is just the Mpemba effect.

VI. CONCLUSIONS

In this work we have studied several variants of the Lindblad equation to describe the dissipative dynamics in presence of phase coexistence. In particular we have considered the exactly-solvable fully-connected quantum Ising model with two and four spin-exchange,
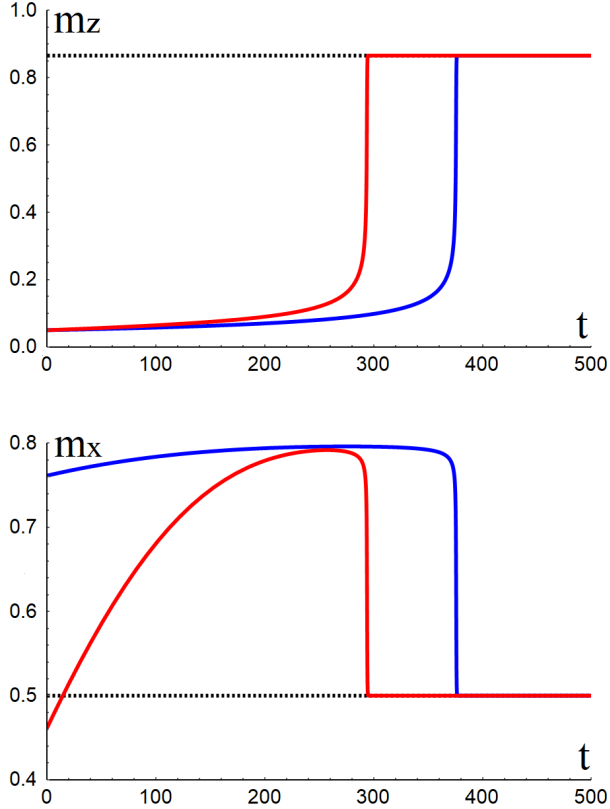
FIG. 6. Dissipative dynamics of the Hamiltonian (4) in case 1 with $J_2 = J_4 = 1$ and $h_x = 2.5$, see phase diagram in panel a) Fig. 3, after a sudden quench of temperature from T_i to $T_f = 0.002 \ll T_i$. Blue and red lines refer to $T_i = 2.5$ and $T_i = 5$, respectively. Top panel: longitudinal magnetisation m_z. Bottom panel: transverse magnetisation m_x. We observe that the initially hotter system (red lines) reaches the equilibrium value of magnetisation faster than the colder one (blue lines).

whose phase diagram is the prototype of a symmetry-breaking quantum first order transition. We have found that a sound dissipative dynamics is recovered only when the Lindblad equation involves jump operators defined in each of the coexisting phases, whether stable or metastable. Applying such equation to the fully-connected quantum Ising model, we are able to describe also intriguing non-equilibrium phenomena, like the Mpemba effect.

[1] J. G. Leidenfrost, *A Tract About Some Qualities of Common Water* (Herman Ovenius, Universal Booksellers, Duisburg on Rhine, 1756).

[2] M. M. Renfrew, Journal of Chemical Education **68**, A48 (1991).

[3] E. Mpemba and D. Osborne, Physics Education **4**, 172 (1969).

[4] H. C. Burridge and P. F. Linden, Scientific Reports **6**, 37665 (2016).

[5] Y. H. Ahn, H. Kang, D. Y. Koh, and H. Lee, Korean Journal of Chemical Engineering **33**, 1903 (2016).

[6] P. Chaddah, S. Dash, K. Kumar, and A. Banerjee, arXiv:1011.3598 (2010).

[7] A. Lasanta, F. Vega Reyes, A. Prados, and A. Santos, Phys. Rev. Lett. **119**, 148001 (2017).

[8] M. Baity-Jesi, E. Calore, A. Cruz, L. A. Fernandez, J. M. Gil-Narvion, A. Gordillo-Guerrero, D. Iniguez, A. Lasanta, A. Maiorano, E. Marinari, V. Martin-Mayor, J. Moreno-Gordo, A. Munoz-Sudupe, D. Navarro, G. Parisi, S. Perez-Gaviro, F. Ricci-Tersenghi, J. J. Ruiz-Lorenzo, S. F. Schifano, B. Seoane, A. Tarancon, R. Tripiccione, and D. Yllanes, arXiv:1804.07569 (2018).

[9] X. Zhang, Y. Huang, Z. Ma, Y. Zhou, J. Zhou, W. Zheng, Q. Jiang, and C. Q. Sun, Phys. Chem. Chem. Phys. **16**, 22995 (2014).

[10] I. Firth, Physics Education **6**, 32 (1971).

[11] G. S. Kell, American Journal of Physics **37**, 564 (1969).

[12] M. Vynnycky and S. Kimura, International Journal of Heat and Mass Transfer **80**, 243 (2015).

[13] D. Auerbach, American Journal of Physics **63**, 882 (1995).

[14] S. Esposito, R. D. Risi, and L. Somma, Physica A: Statistical Mechanics and its Applications **387**, 757 (2008).

[15] D. G. Fahrenheit, "Experimenta & observationes de congelatione aquae in vacuo factae," Philosophical Transactions.

[16] S. Wald and M. Henkel, Journal of Physics A: Mathematical and Theoretical **49**, 125001 (2016).

[17] G. Prataviera and S. Mizrahi, Revista Brasileira de Ensino de Fisica **36**, 01 (2014).

[18] T. c. v. Prosen and I. Pižorn, Phys. Rev. Lett. **101**, 105701 (2008).

[19] H. De Raedt, F. Jin, M. I. Katsnelson, and K. Michielsen, Phys. Rev. E **96**, 053306 (2017).

[20] J. P. Santos and G. T. Landi, Phys. Rev. E **94**, 062143 (2016).

[21] S. Bhattacharya, A. Misra, C. Mukhopadhyay, and A. K. Pati, Phys. Rev. A **95**, 012122 (2017).

[22] T. Prosen and M. Žnidarič, Journal of Statistical Mechanics: Theory and Experiment **2009**, P02035 (2009).

[23] A. Karabanov, D. C. Rose, W. Köckenberger, J. P. Garrahan, and I. Lesanovsky, Phys. Rev. Lett. **119**, 150402 (2017).

[24] H. Schwager, J. I. Cirac, and G. Giedke, Phys. Rev. A **87**, 022110 (2013).

[25] G. Lindblad, Comm. Math. Phys. **48**, 119 (1976).

[26] P. Pearle, European Journal of Physics **33**, 805 (2012).

[27] P. Nalbach, Phys. Rev. A **90**, 042112 (2014).

[28] H. C. F. Lemos and T. c. v. Prosen, Phys. Rev. E **95**, 042137 (2017).

[29] M. Žnidarič, Phys. Rev. A **91**, 052107 (2015).

[30] L. Arceci, S. Barbarino, R. Fazio, and G. E. Santoro, Phys. Rev. B **96**, 054301 (2017).

[31] A. Das, K. Sengupta, D. Sen, and B. K. Chakrabarti, Phys. Rev. B **74**, 144423 (2006).

[32] F. Minganti, A. Biella, N. Bartolo, and C. Ciuti, Phys. Rev. A **98**, 042118 (2018).

[33] B. H. Teng and H. K. Sy, Europhysics Letters (EPL) **73**, 601 (2006).

[34] L. Arceci, S. Barbarino, D. Rossini, and G. E. Santoro, Phys. Rev. B **98**, 064307 (2018).

[35] O. Penrose and J. L. Lebowitz, in *Fluctuation Phenomena*, edited by E. W. Montroll and J. L. Lebowitz (Elsevier, 1987) pp. 7–293.

[36] K. Macieszczak, M. u. u. u. u. Guţă, I. Lesanovsky, and J. P. Garrahan, Phys. Rev. Lett. **116**, 240404 (2016).

[37] D. C. Rose, K. Macieszczak, I. Lesanovsky, and J. P. Garrahan, Phys. Rev. E **94**, 052132 (2016).

[38] N. Lang and H. P. Büchler, Phys. Rev. A **92**, 012128 (2015).

[39] J. Lauwers and A. Verbeure, Journal of Physics A: Mathematical and General **34**, 5517 (2001).

[40] L. Del Re, M. Fabrizio, and E. Tosatti, Phys. Rev. B **93**, 125131 (2016).

[41] M. M. Wauters, R. Fazio, H. Nishimori, and G. E. Santoro, Phys. Rev. A **96**, 022326 (2017).

[42] S. L. Adler, Physics Letters A **265**, 58 (2000).

[43] A. Redfield, in *Advances in Magnetic Resonance*, Advances in Magnetic and Optical Resonance, Vol. 1, edited by J. S. Waugh (Academic Press, 1965) pp. 1 – 32.

[44] C. Müller and T. M. Stace, Phys. Rev. A **95**, 013847 (2017).

[45] L. M. Sieberer, M. Buchhold, and S. Diehl, Reports on Progress in Physics **79**, 096001 (2016).